

## Interaction of EDNA with Proton-A DFT Treatment

Lemi Türker

Middle East Technical University, Department of Chemistry Üniversiteler, Eskişehir Yolu No:1, 06800

Çankaya/Ankara Turkey

lturker@gmail.com, lturker@metu.edu.tr

### Abstract.

A composite of EDNA, with proton in vacuum have been **considered** within the constraints of density functional theory at the levels of B3LYP/6-31++G(d,p) (restricted and unrestricted) and  $\omega$ B97X-D/6-311+G(d,p). The results of structure optimization indicated that unexpectedly hydrogen molecule production occurs by the interaction of proton and a methylenic hydrogen of EDNA resulting a carbocation formation on the explosive molecule. The remnant of the nitramine molecule is stabilized partly by the nearby nitro oxygen atoms through space. The calculated IR and UV- VIS spectra of the species were obtained and discussed.

**Key words:** EDNA, Haleite, Explosives, Proton, Nitramine, DFT.

### 1. Introduction

EDNA is also named as Haleite, N,N'-dinitroethylene diamine, 1,2-dinitrodiaminoethane

(C<sub>2</sub>H<sub>6</sub>N<sub>4</sub>O<sub>4</sub>). It has energy of formation and enthalpy of formation values of -576 kJ/kg and -691.6 kJ/kg, respectively [1]. Its oxygen balance is -32% so it is mostly used together with some oxidizing agents. It is characterized with 37.33 % nitrogen content, crystallizes as white orthorhombic crystals (d:1.71 g/cm<sup>3</sup>)[1]. EDNA is an explosive that combines the properties of a high explosive like TNT [2]. Indeed, it is more powerful than TNT and slightly less powerful than RDX [3]. It has high brisance and comparatively low sensitivity to impact (8 Nm) [1,2] and at the same time so readily explodes by heat. Its explosion temperature is relatively low (melts with decomposition at 177.30 °C) approaching that of mercury fulminate or nitroglycerine [2]. It possesses detonation velocity (confined) value of 7570 m/s [1]. EDNA acts as a dibasic acid and forms various neutral salts which also have some explosive properties [1].

Heat sensitization of EDNA (beside some other explosives) was investigated along time ago [4] . Thermochemical data including EDNA (Haleite) relative to the constituents of propellants were reported [5]. Its decomposition mechanism depending on the properties of the medium was studied [6]. Its crystallographic data were published By McCrone [7]. The use of co-crystallizations is emerging as a new avenue for modifying the solid-state properties of a wide range of high-value chemicals. Co-crystals of ethylenedinitramine (EDNA) has been prepared by crystal engineering [8]. Insensitive EDNA/DAT Co-crystal was investigated by Zeman and coworkers [9]. Spaeth and Winning managed to produce ethylene dinitramine pellets by using some additives to obtain ameliorated performance [10]. The general use of EDNA is restricted due to its relatively high chemical reactivity, caused by the presence of two highly acidic protons. Thus, EDNA is corrosive and can, over time, react with metals and metal salts which may in turn produce brand new and unknown materials with completely unpredictable properties [8]. Theoretical calculations of hot-spot initiation in explosives, including EDNA, was performed by Bruckman and Guillet [11].

On the other hand, cosmic rays have great penetrating power. The intensity of them varies with latitude. Cosmic rays consist largely of the nuclei of elements of low atomic weight, protons being the most abundant type [12]. The hard component of cosmic rays is  $\mu$ -mesons produced in flight by  $\pi$ -meson decay. The soft component which is not very penetrating consists of photons, electrons and positrons [12-16].

In the present study, EDNA+proton composite (EDNA+p) system has been considered in vacuum conditions within the constraints of density functional theory (DFT).

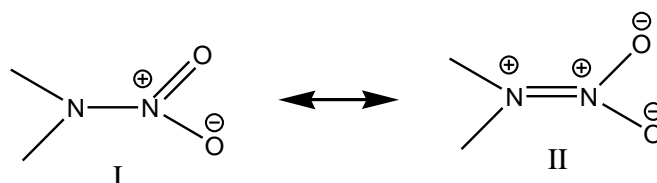
## 2. Method of calculation

Structure optimizations of all the species, leading to energy minima were initially achieved by using MM2 method followed by semi-empirical PM3 self-consistent fields molecular orbital (SCF MO) method [17,18] (at the restricted level [19,20]. The subsequent optimizations have been achieved at Hartree-Fock level using various basis sets hierarchically. Then, the structure optimizations were managed within the framework of density functional theory [21,22], finally at the levels of both B3LYP /6-31++G(d,p) [19] and  $\omega$ B97X-D/6-311+G(d,p) [23,34]. For the open-shell systems or for special purposes unrestricted DFT calculations were performed. The exchange term of B3LYP consists of hybrid Hartree-Fock and local spin density (LSD) exchange functions with Becke's gradient correlation to LSD exchange [22,25]. Note that the correlation term of B3LYP consists of the Vosko, Wilk, Nusair (VWN3) local correlation functional [26] and Lee, Yang, Parr (LYP) correlation correction functional [27].

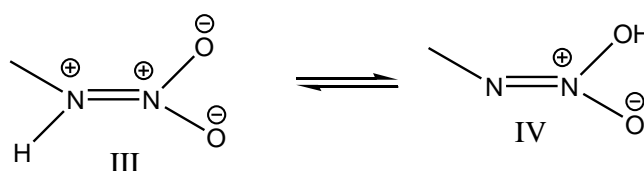
The vibrational analyses were also done. The total electronic energies are corrected for the zero-point vibrational energy (ZPE). The stationary points to energy minima were proved in all the cases by calculation of the second derivatives of energy with respect to the atom coordinates. The normal mode analysis for each structure yielded no imaginary frequencies for the  $3N-6$  vibrational degrees of freedom, where  $N$  is the number of atoms in the system. This indicates that the structure of each system corresponds to at least a local minimum on the potential energy surface. All these calculations were done by using the Spartan 06 package program [28].

## 3. Results and discussion

EDNA is a nitramine type explosive. Mesomerically electron withdrawing nitro group and adjacent electron donating amino group dictate most of the characteristic behavior of EDNA. The following mesomeric structures are to be considered for the nitramine group.



Two adjacent positively charged nitrogen atoms in structure II, may initiate a 1,3 tautomerism if it is structure allows.



On the other hand, when a charged particle approaches a molecule, the electric field generated by its presence disturbs the electric field around the neutral molecule. This is a time-dependent dynamic process. As the charged particle gets slower and slower its ionization density (ionization along the particle's path, the Bragg's curve) increases [29]. However, prior to or just after the spark breakdown (very small  $\Delta t$  seconds earlier or later) the whole picture can be simplified as the molecule and a charged-particle (composite system) at the equilibrium geometry. Obviously, due to the polarization effects, bond lengths and angles of the molecule adapt themselves to minimize the energy of the composite system. It is known that any form of nuclear radiation (charged particles, neutrons or electromagnetic radiation) directly or indirectly produces ionization

and certain chemical changes in its passage through matter [15,29]. Positively charged particles, engender rather strong electric field around them to initiate ionization of nearby molecules.

### 3.1. Bond lengths and distances

Figure 1 shows the optimized structures and the resultant bond lengths/distances calculated at two different DFT levels and the direction of dipole moment vector. Note that the levels of calculations have two different basis sets and functionals in order to visualize whether the bond lengths/ distances are independent from the method of calculations or not. The results reveal that in each case, one of the methylenic hydrogen-carbon bonds is highly elongated implying its cleavage. The distance between the originally proton and originally methylenic hydrogen is 0.745 Å (B3LYP/ 6-31++G(d,p)) and 0.747 Å ( $\omega$ B97X-D/ 6-311+G(d,p)) suggesting some strong interaction (bond formation) between them.

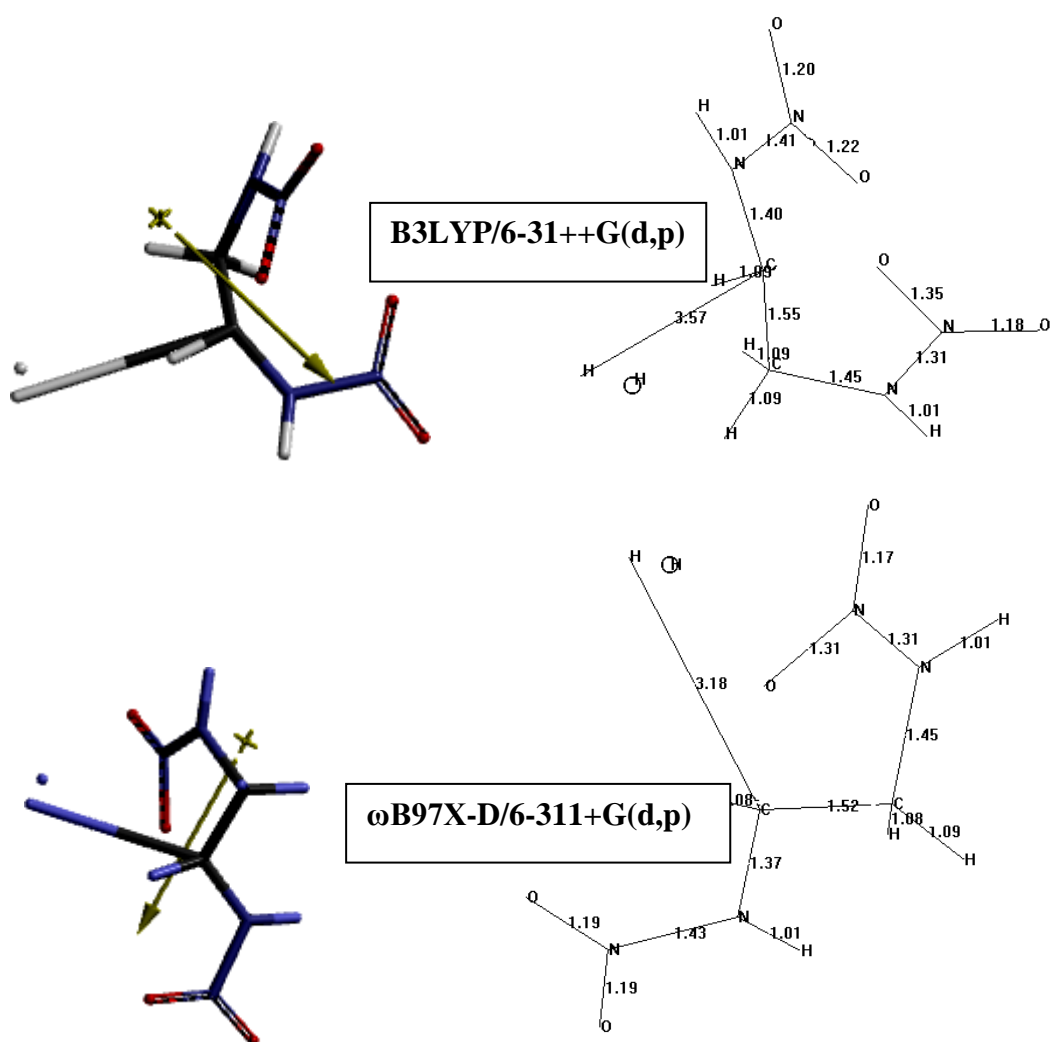
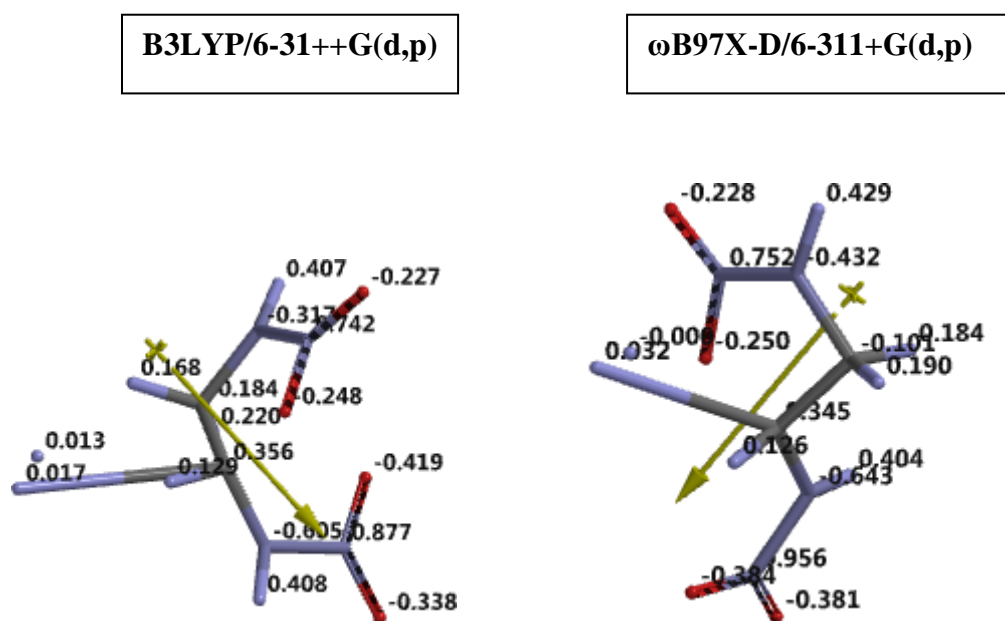


**Figure 1.** Optimized structure and bond lengths for EDNA+p system.

### 3.2. Charges

The ESP charges on EDNA+p system is shown in Figure 2. The ESP charges are obtained by the program based on a numerical method (CHELP algorithm) that generates charges that reproduce the electrostatic potential field from the entire wavefunction [28]. In this algorithm the charges at the atoms are chosen to best describe the external field surrounding the molecule. Ideally this area should include everything outside of the Van der Waal radii. In practice, a shell surrounding the atoms having a thickness of 5.5 au is chosen for ESP calculations.

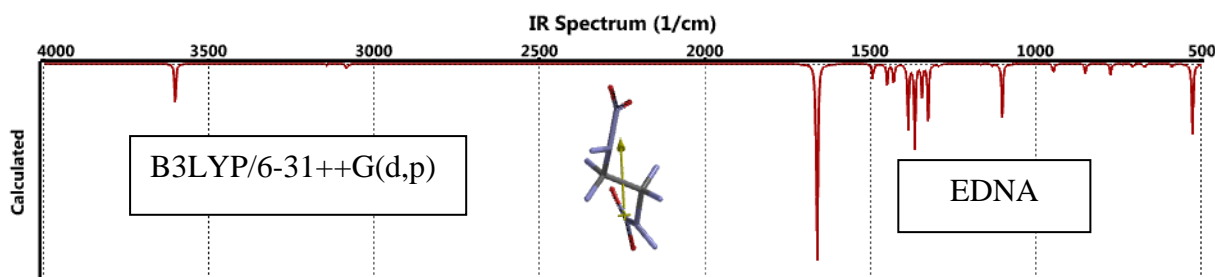
The hydrogen originally in protonic form, and similarly the methylenic hydrogen have very minute charges or nil. The affected methylenic carbon has quite big partial positive charge (see Figure 2).



**Figure 2.** The ESP charges (esu) on atoms of EDNA+p system.

### 3.3. IR spectra

Figure 3 displays the IR spectra of EDNA as well as the composite, EDNA+p system. At the B3LYP/6-31++G(d, p) level, the peak at  $1665\text{ cm}^{-1}$  is the nitramine N-H bending coupled with asymmetric N-O stretching of EDNA which occurs at  $1718\text{ cm}^{-1}$  and  $1771\text{ cm}^{-1}$  in EDNA+p composite system. These peaks at  $\omega$ B97X-D/6-311+G(d,p) level of calculations are very closely spaced at  $1797\text{ cm}^{-1}$ . Also, the N-H stretching peaks are not well resolved in this level of calculations as compared to B3LYP/6-31++G(d, p) level. The nitramine N-H stretching occurs in the region of ca.  $3554\text{--}3571\text{ cm}^{-1}$ .



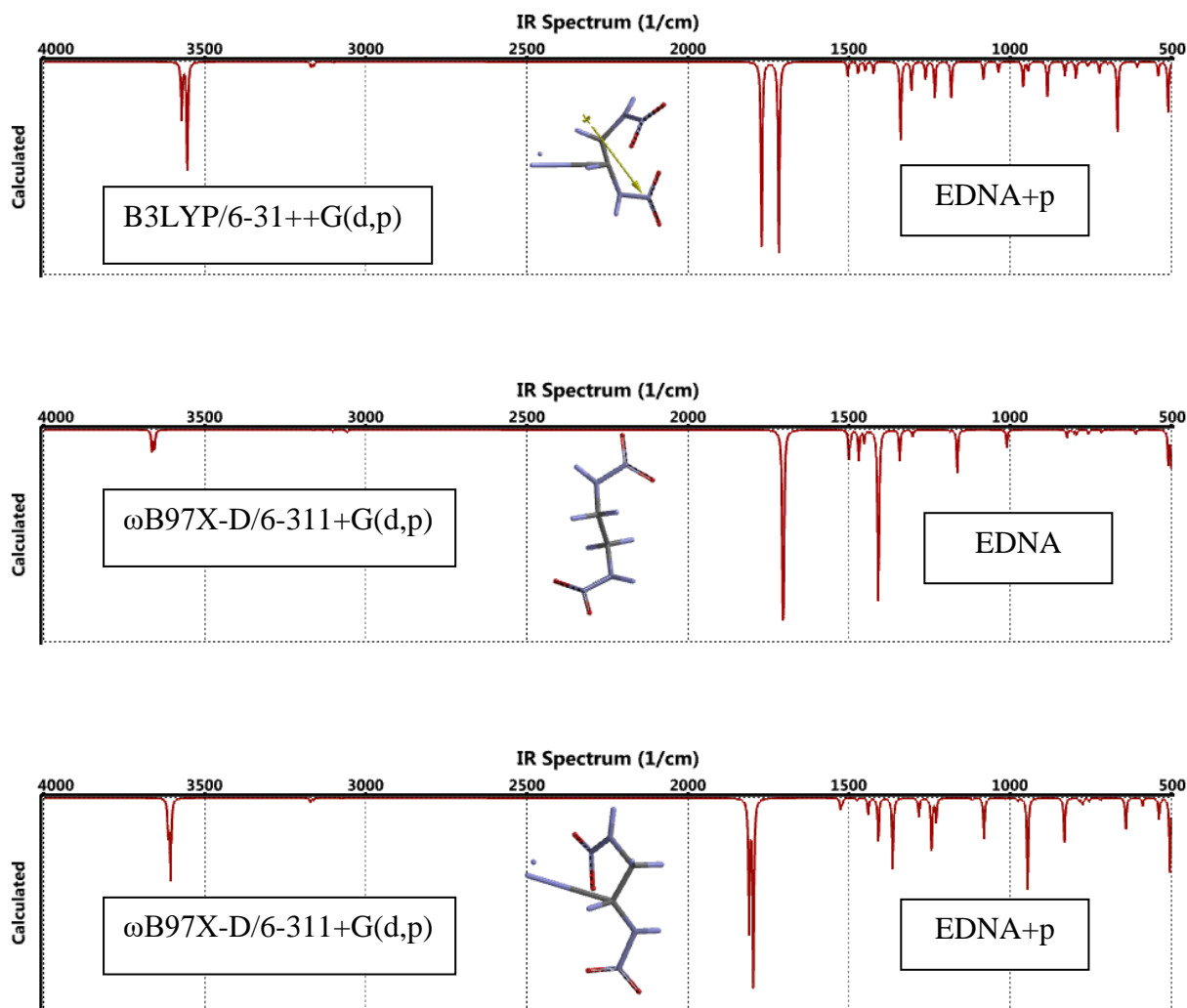


**Figure 3.** IR spectrum of EDNA and EDNA+p system.

### 3.4. Molecular orbital energies and UV-VIS spectra

Figure 4 shows some of the molecular orbital energy levels of EDNA and the composite system EDNA+p. As seen in the figure and Table 1, the presence of proton in the composite system lowers both the HOMO and LUMO energy levels. The effect of this energy lowering on the interfrontier molecular orbital energy gap ( $\Delta\epsilon$ ,  $\epsilon_{\text{LUMO}} - \epsilon_{\text{HOMO}}$ ) is narrowing of the gap. Consequently, the UV-VIS spectrum of the composite system is expected to exhibit a bathochromic shift to visible region of the spectrum.

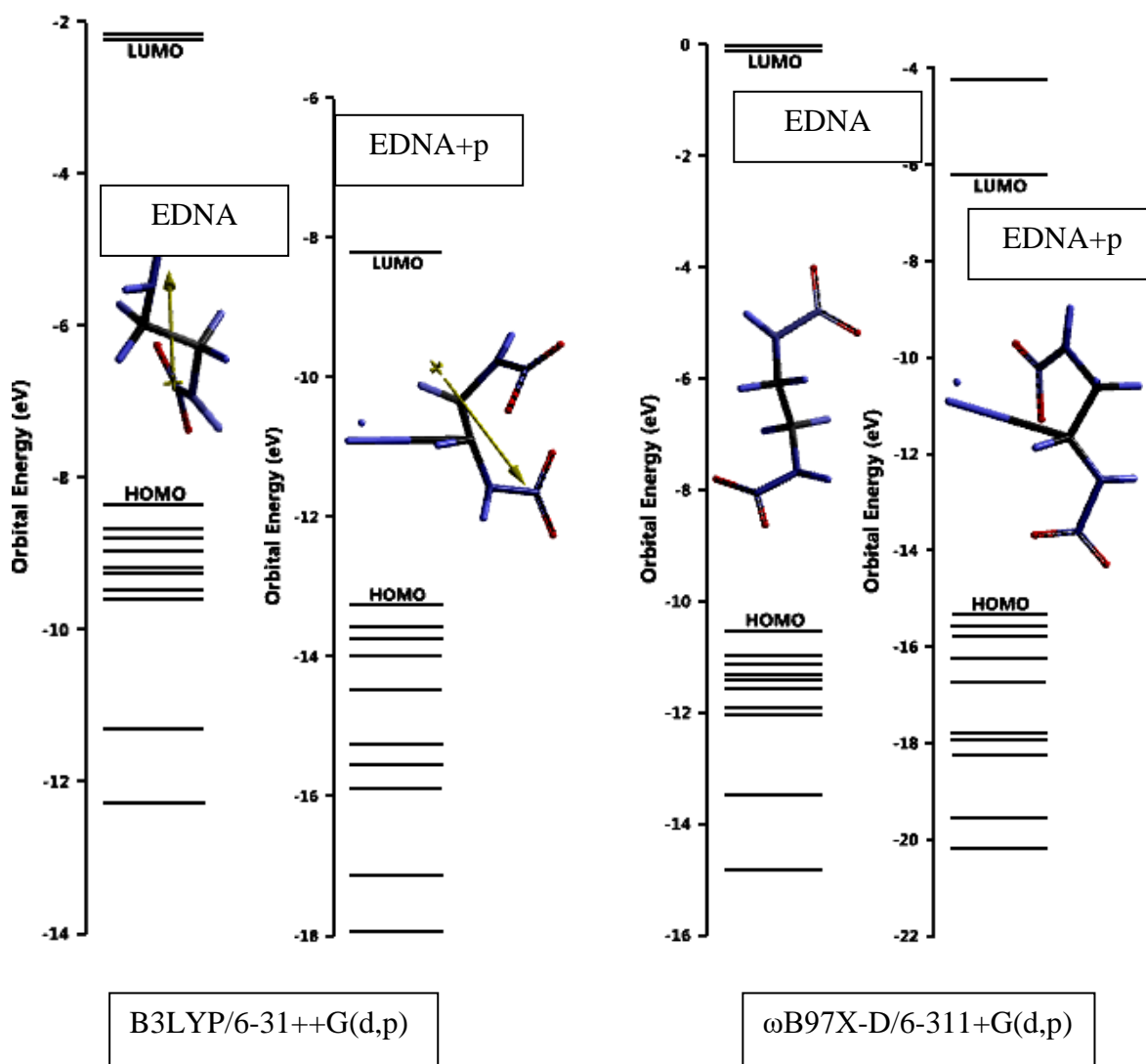


**Figure 4.** Some of the molecular orbital energy level of EDNA and EDNA+p system.

**Table 1.** The HOMO, LUMO energies and FMO gaps for the systems considered.

System	$\epsilon_{\text{HOMO}}$	$\epsilon_{\text{LUMO}}$	$\Delta\epsilon$
EDNA	-806.42 (-1016.31)	-215.27 (-10.50)	591.15 (1005.81)
EDNA+p	-1279.26 (-1478.88)	-792.63 (-599.28)	486.63 (879.6)

Energies in kJ/mol. B3LYP/6-31++G(d,p) and B97X-D/6-311+G(d,p) (in parenthesis) levels.

HOMO

LUMO

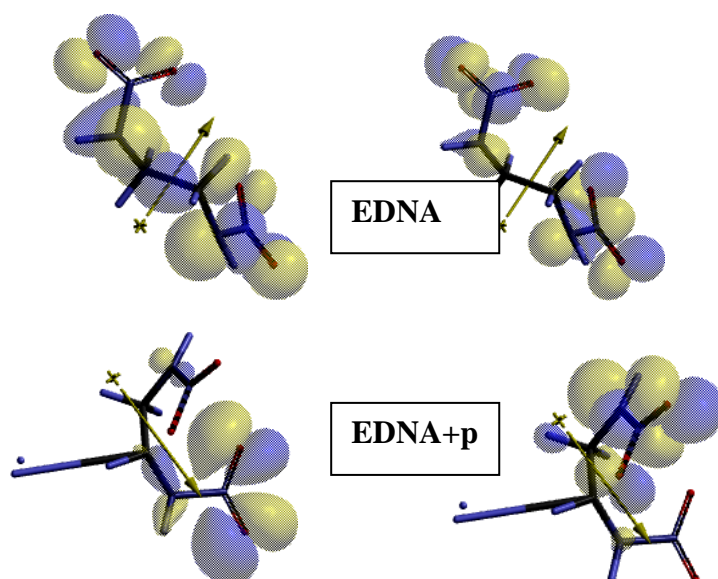


**Figure 5.** The HOMO and LUMO patterns for the systems considered (B3LYP/6-31++G(d,p)).

Figure 6 shows the UV-VIS spectra (time dependent) of EDNA and EDNA+p composite system. It is to be noted that B3LYP/6-31++G(d,p) level of calculations yield a spectrum closer to visible region as compared to  $\omega$ B97X-D/6-311+G(d,p) level. Note that, as mentioned above, the UV-VIS spectrum of the composite system is expected to exhibit a bathochromic shift to visible region of the spectrum from the direct consequence of narrowing of the FMO gap (see Table 1). However, the calculated UV-VIS spectra at the level of  $\omega$ B97X-D/6-311+G(d,p) is insensitive to the presence of proton compared to EDNA system. This might be because of the limited number of molecular orbitals considered in spectral calculations for the sake of minimizing the calculation expenses.

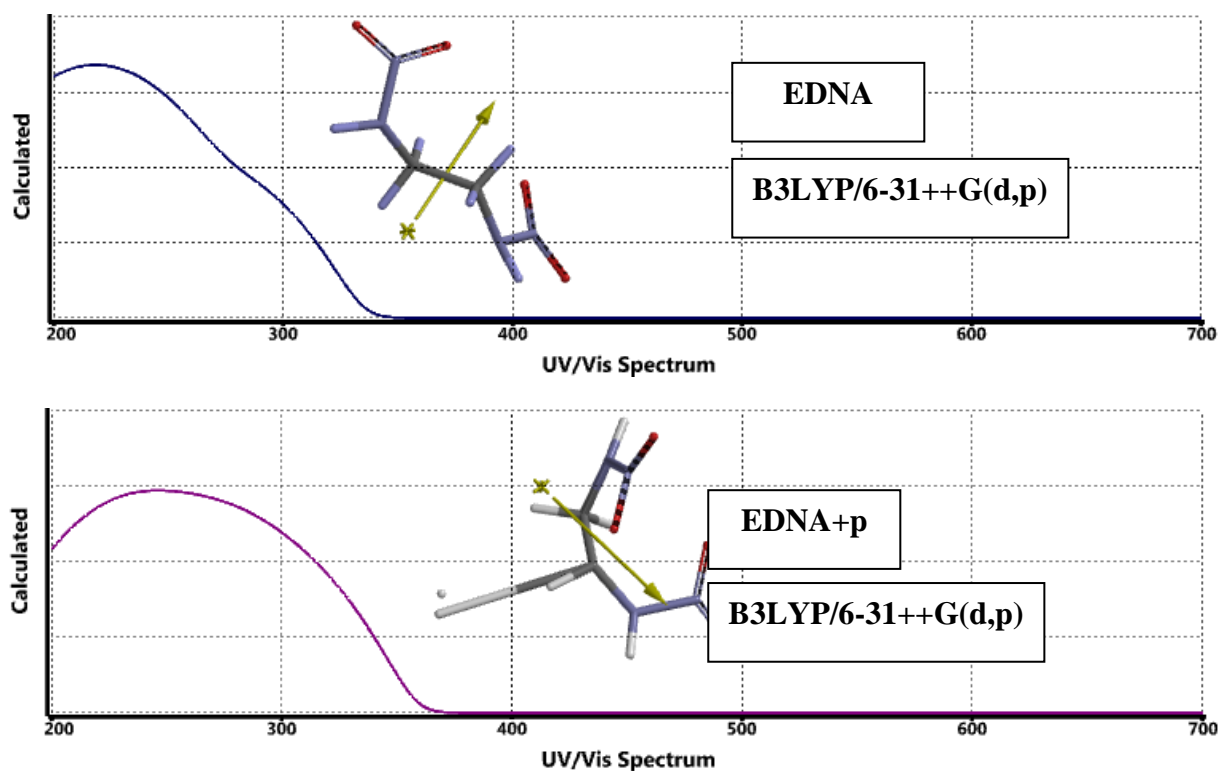


Figure 6 contd.

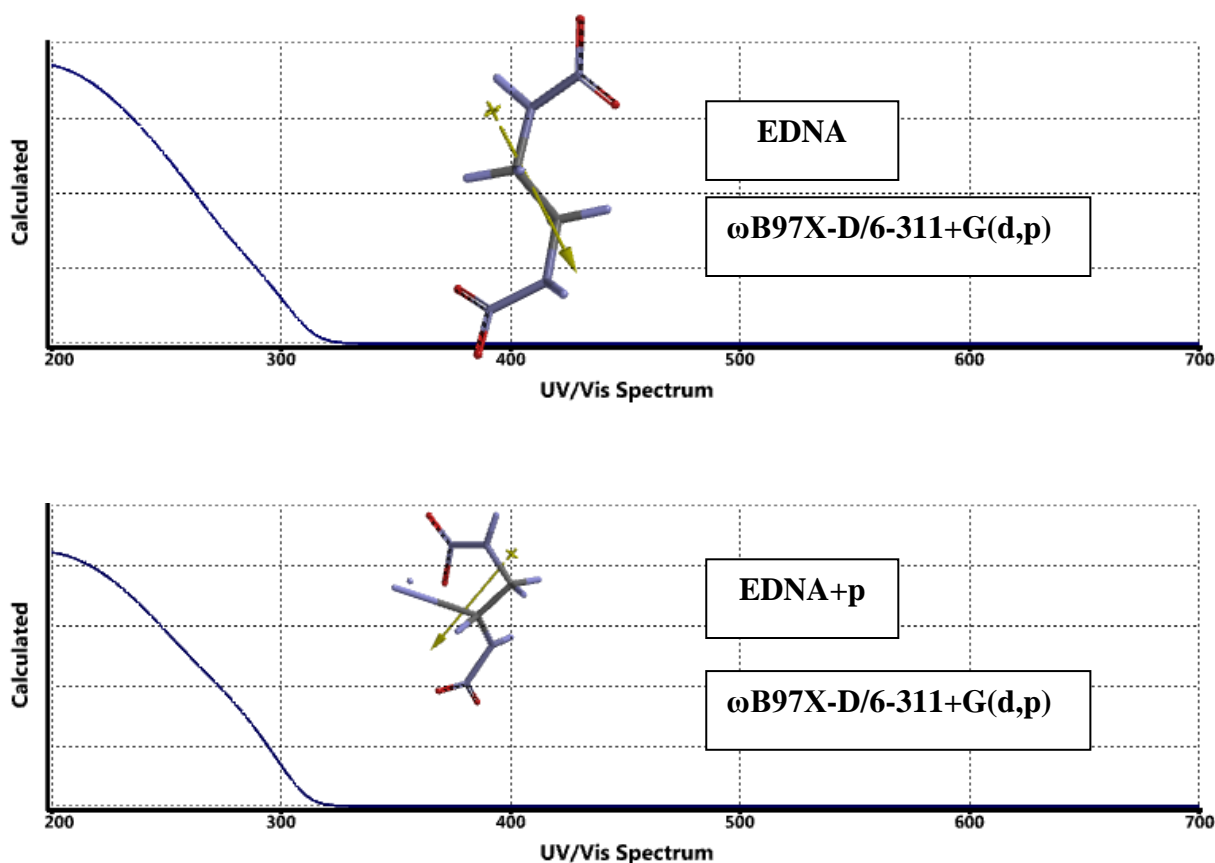


Figure 6. UV-VIS spectrum of systems presently considered.

### 3.5. The mechanism of interaction

For the mechanism studies, the proton and the methylenic hydrogen affected by the proton are removed from the optimized structure of EDNA+p system. Then, calculations were performed by adopting the unrestricted formalism (UB3LYP/6-31+G(d,p)). These types of structures are indicated as EDNA-H<sub>2</sub>.

Although, proton is positively charged and EDNA has NO<sub>2</sub> groups which have negatively charged oxygen atoms, the proton nearby EDNA seems to prefer the covalently bound methylenic hydrogen of EDNA. Figure 7 shows the optimized structures of the systems considered for the mechanism of interaction. All the optimizations in this section were carried out at the unrestricted level, irrespective of closed or open shell systems have been considered. Note that the main skeleton and the direction of dipole moments in the cases of EDNA+p and EDNA cation are quite similar.



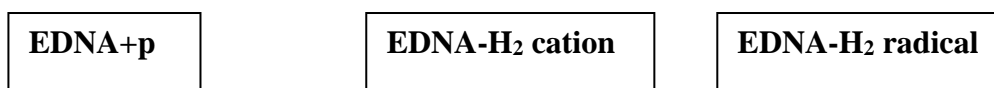


**Figure 7.** Optimized structures for the species considered (UB3LYP/6-31++G(d,p)).

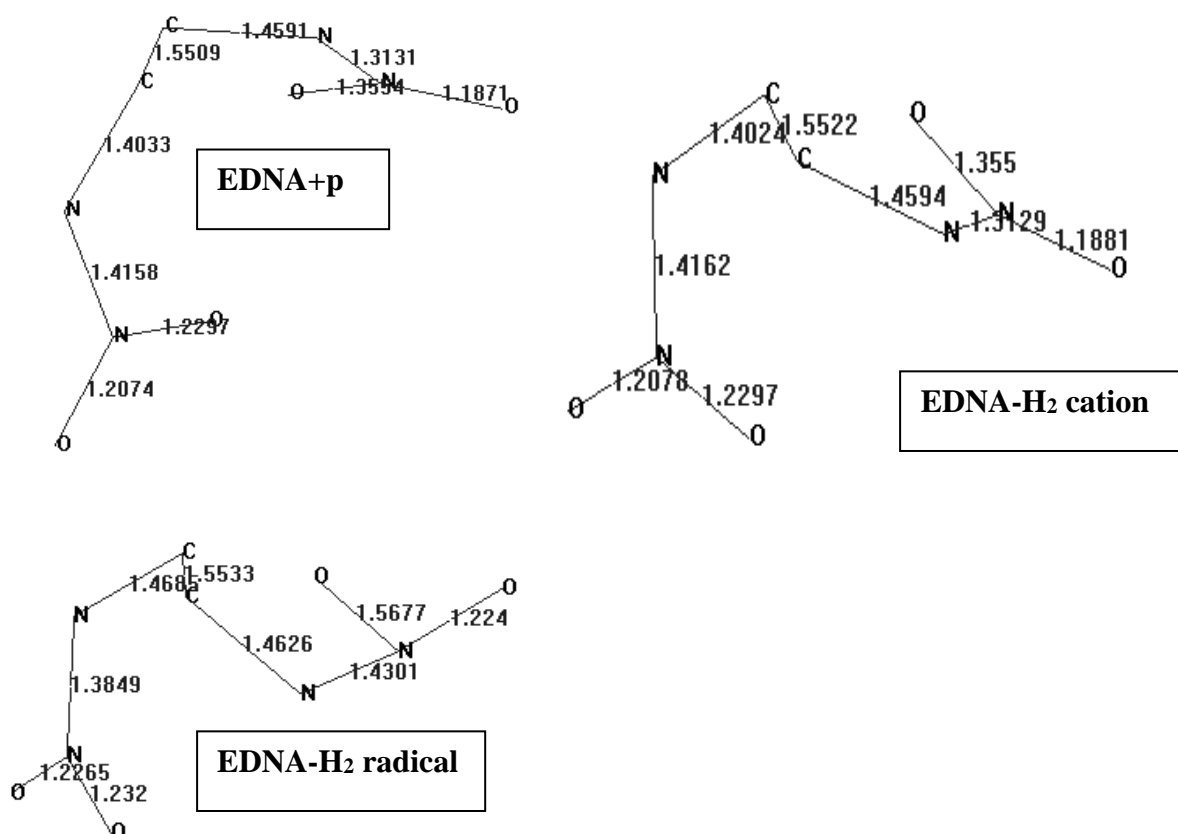
Table 2 shows various energies of the systems considered obtained either restricted or unrestricted manner.

**Table 2.** Various energies of the species considered.

Specie	E	ZPE	E <sub>c</sub>
EDNA*	-1574071.20	305.73	-1573765.47
EDNA+p*	-1574775.12	308.83	-1574466.29
EDNA+p**	-1574775.12	308.81	-1574466.31
EDNA-H <sub>2</sub> cation**	-1571677.29	279.20	-1571398.09
EDNA-H <sub>2</sub> radical**	-1572366.70	273.75	-1572092.95

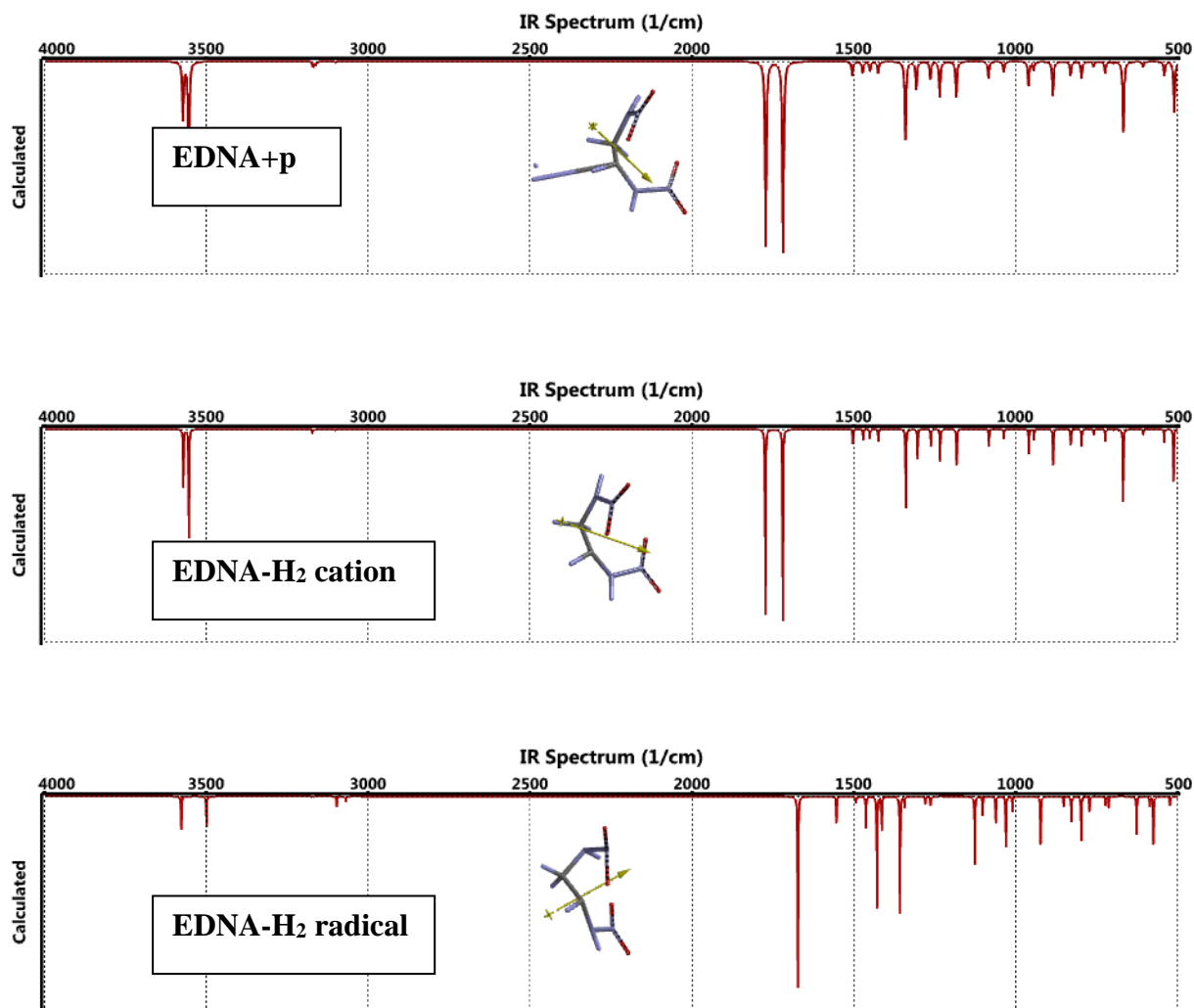
Energies in kJ/mol. \* B3LYP/6-31++G(d,p), \*\* UB3LYP/6-31++G(d,p)

Figure 8 shows the bond lengths of EDNA+p and cation and radical obtained after the removal of H<sub>2</sub> from EDNA+p system.



**Figure 8.** Bond lengths in the species considered (UB3LYP/6-31++G(d,p) level, hydrogens are omitted).

Figure 9 displays the IR spectra of various species considered in this section. Note the high similarity between the spectrums of EDNA+p and EDNA-H<sub>2</sub> cation. In these systems, the peaks at 1771 cm<sup>-1</sup> and 1718 cm<sup>-1</sup> are the nitramine N-H bending coupled with asymmetric N-O stretching of nitramine groups present in EDNA.



**Figure 9.** IR spectra of the species considered (UB3LYP/6-31++G(d,p)).

Figure 10 shows the calculated (time dependent, TDDFT) UV-VIS spectra (UB3LYP/6-31++G(d,p)) of the species considered. A high similarity between the UV-VIS spectrums of EDNA+p and EDNA-H<sub>2</sub> cation are observed. It shows that in the composite system, methylenic hydrogen of EDNA leaves of the molecule in pro-hydride form to combine with the proton nearby and EDNA remnant is left in the cationic form.

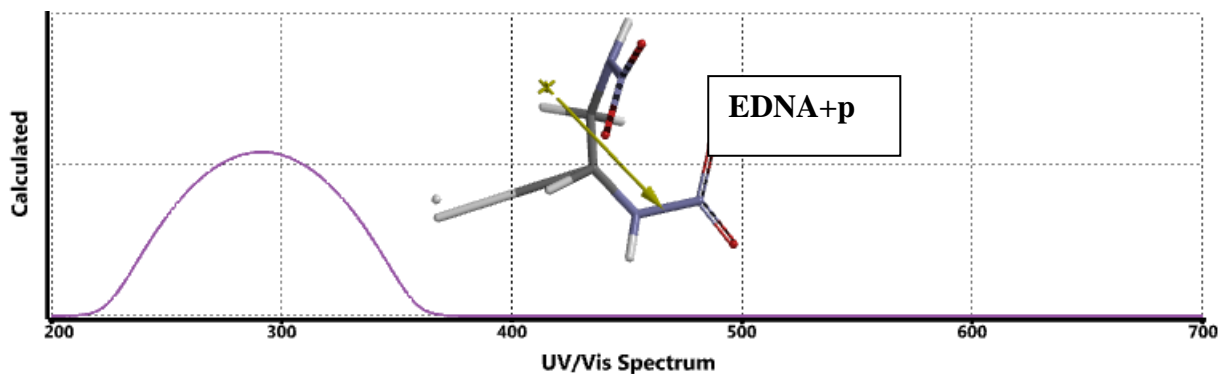


Figure 10 contd.

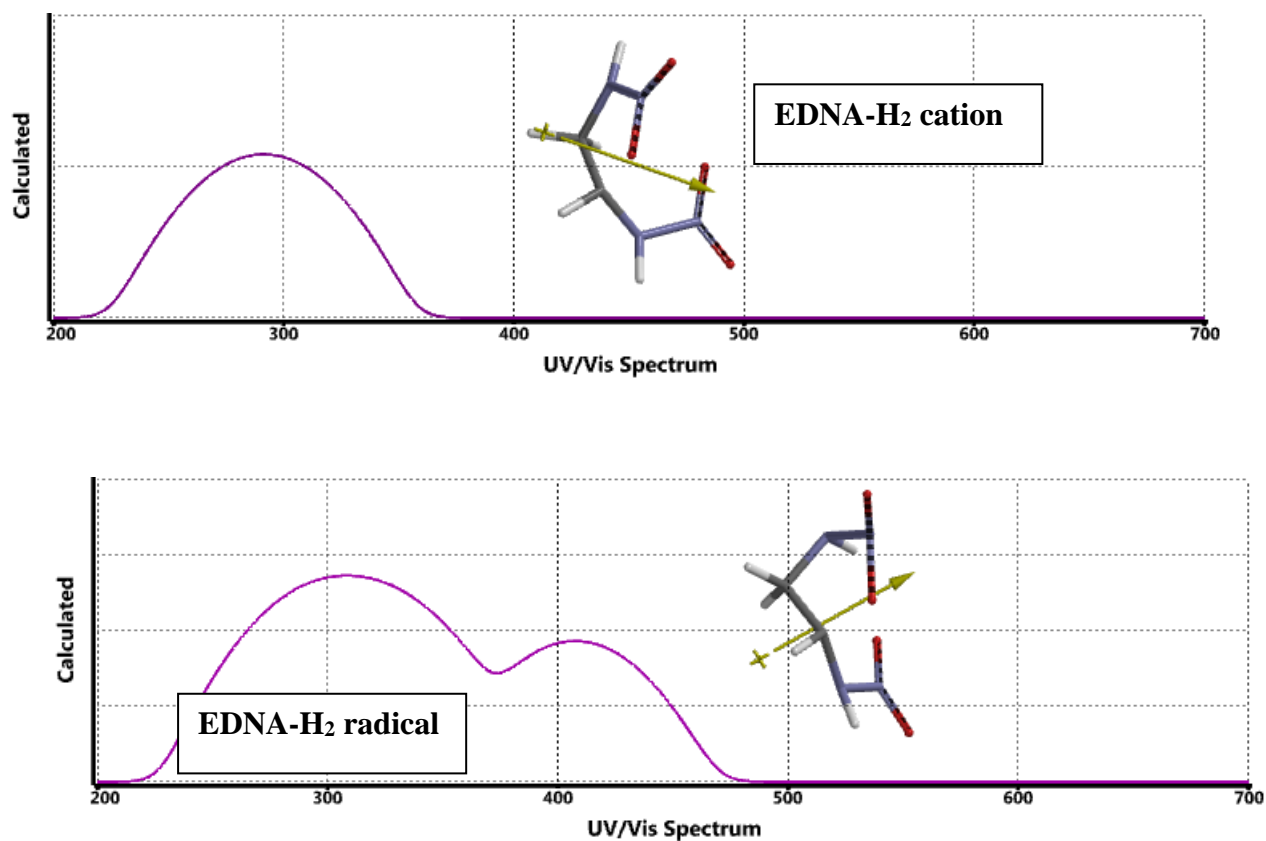
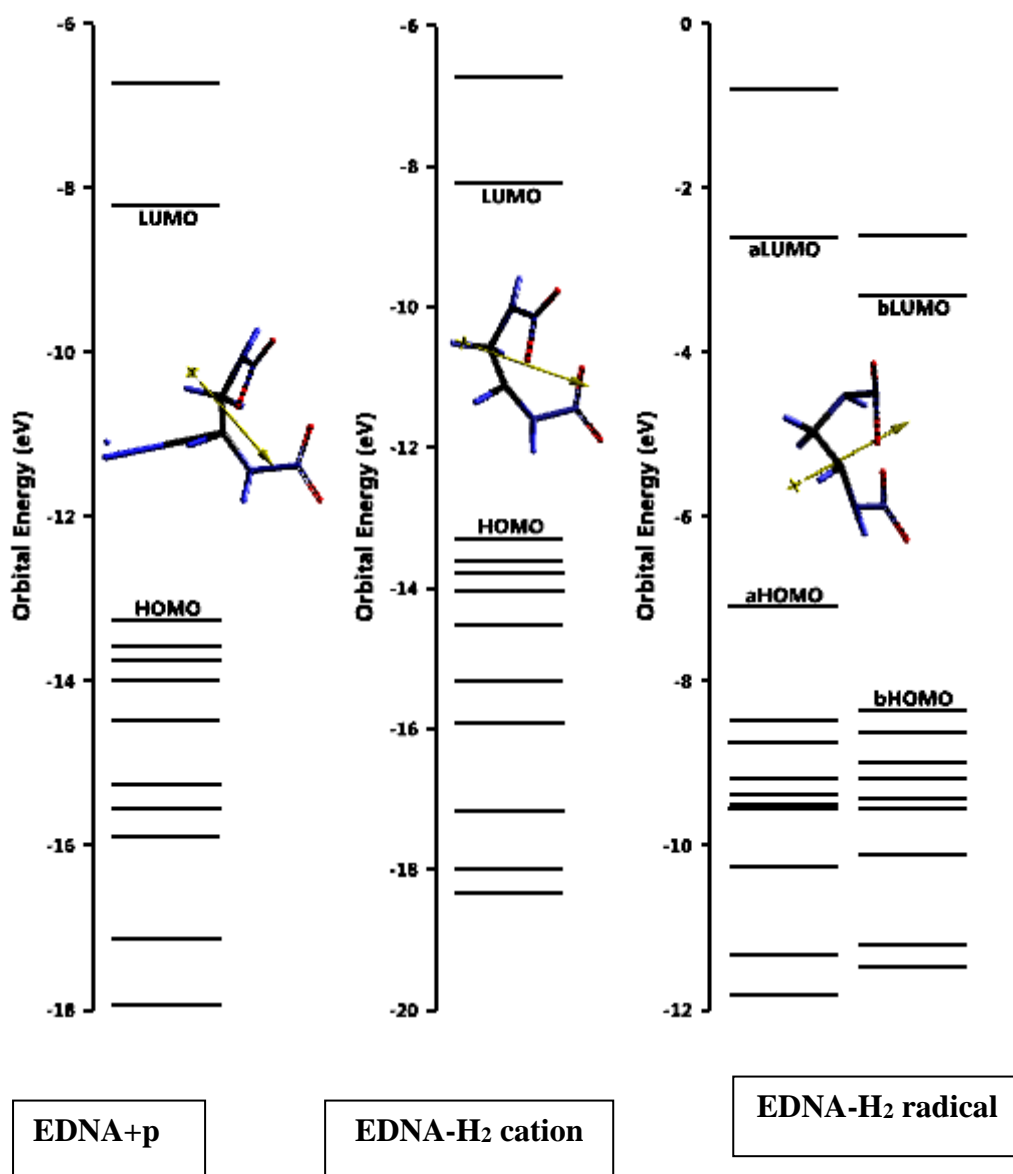
**Figure 10.** UV-VIS spectra of the species considered (UB3LYP/6-31++G(d,p)).

Figure 11 shows some of the molecular orbital energy spectra of the species considered (UB3LYP/6-31++G(d,p)) in this section. Note that the calculations are unrestricted thus for open shell systems  $\alpha$ - and  $\beta$ -type orbitals arise.



**Figure 11.** Some of the molecular orbital energy spectra of the species considered (UB3LYP/6-31++G(d,p)).

## Conclusion

According to the present level of DFT calculations, exposure of EDNA to cosmic protons from the primary cosmic rays result in H<sub>2</sub> formation in which one of the H atoms originates from the methylene moiety present in the structure of EDNA. The present study shows that in space (vacuum), chemistry (at least for EDNA) could be quite unexpected and different from aqueous or solution chemistry. Presently, only the effect of a static proton nearby EDNA molecule has been modeled. Note that cosmic protons have high speed and the electric field generated by them has dynamic features as well. Anyhow, the present study focuses attention to the stability of energetic materials to be used in space conditions.

## References

1. Meyer R, Köhler J, Homburg A, Explosives. Weinheim, Wiley-VCH, 2002.
2. Military Explosives, TM 9-1300-214. Headquarters of the Army, Washington, DC, Sep 25, 1990.

3. Wijethunga T.K, Aakeroy C.B, Desper J, Crystal engineering of energetic materials: Co-crystals of ethylenedinitramine (EDNA), 49th Midwest Regional Meeting of the American Chemical Society, Columbia, MO, United States, November 12-15 (2014), MWRM-333.
4. Jones M.M, Jackson H.J, Heat sensitization of explosives, *Explosivstoffe*, 7, (1959) 177- 83.
5. Tavernier P, Thermochemical data relative to the constituents of propellants, *Memorial des Poudres*, 38 (1956) 301-36.
6. Tomlinson W.R., Jr, Decomposition of Haleite (ethylenedinitramine), *Journal of Organic Chemistry*, 17 (1952) 648-68.
7. McCrone W.C, Crystallographic data. Ethylenedinitramine (Haleite, Edna), *Anal. Chem.*, 24 (1952) 421-2.
8. Aakeröy C.B., Wijethunga T.K., Desper J, Crystal engineering of energetic materials: Co-crystals of ethylenedinitramine (EDNA) with modified performance and improved chemical stability, *Chemistry-A European Journal*. 21(31) (2015) 10921-10921.
9. Khaled H.A, Zeman S, Elbeih A, Synthesis, performance, and thermal behavior of a novel insensitive EDNA/DAT cocrystal, *Zeitschrift für Anorganische und Allgemeine Chemie*, 644(8-9) (2018). DOI: 10.1002/zaac.201800041.
10. Spaeth C.P, Winning C.H, Ethylene dinitramine pellets, (1950), US 767665 19500000.
11. Bruckman H.J., Jr., Guillet J. E, Theoretical calculations of hot-spot initiation in Explosives, *Canadian Journal of Chemistry*, 46 (1968) 3221-3228.
12. Williams J.E, Metcalfe H.C, Trinckle F.E, Lefler R.W, *Modern Physics*. Holt- Rinehart-Wiston, New York, 1968.
13. Ohanian H.C, *Physics*. Norton, NY, 1989.
14. Sears R, Zemansky W, *University Physics*, part 2. Addison-Wesley, Reading, 1963.
15. Friedlander G, Kennedy J.W, Miller J.M, *Nuclear and Radiochemistry*. Wiley- Toppan, Tokyo, 1964.
16. Beiser A, *Concepts of Modern Physics*. McGraw-Hill-Kogakusha, Tokyo, 1967.  
  
Stewart, J.J.P, Optimization of parameters for semiempirical methods I. Method, *J. Comput. Chem.*, 10 (1989) 209-220.  
  
Stewart, J.J.P, Optimization of parameters for semi empirical methods II. Application, *J. Comput. Chem.*, 10 (1989) 221-264.
17. Leach A.R, *Molecular Modeling*. Essex, Longman, 1997.
18. Fletcher P, *Practical Methods of Optimization*. New York, Wiley, 1990.
19. Kohn W, Sham L, Self-consistent equations including exchange and correlation effects, *J Phys Rev.*, 140 (1965) 1133-1138.
20. Parr R.G, Yang W, *Density Functional Theory of Atoms and Molecules*. London, Oxford University Press, 1989.

21. Minenkov Y, Singstad A, Occhipinti G and Jensen V.R, The accuracy of DFT-optimized geometries of functional transition metal compounds: a validation study of catalysts for olefin metathesis and other reactions in the homogeneous phase, *Dalton Trans.*, 41(18) (2012) 5526-41. doi: 10.1039/c2dt12232d. Epub 2012 Mar 20.
22. Kozuch S. and Martin J.M.L, Spin-component-scaled double hybrids: An extensive search for the best fifth-rung functionals blending DFT and perturbation theory, *J. Chem. Theory Comput.*, 34 (2013) 2327-2344.
23. Becke A.D, Density-functional exchange-energy approximation with correct asymptotic Behavior, *Phys Rev A.*, 38 (1988) 3098-3100.
24. Vosko S.H, Vilk L, Nusair M, Accurate spin-dependent electron liquid correlation energies for local spin density calculations: a critical analysis, *Can J Phys.*, 58 (1980) 1200-1211.
25. Lee C, Yang W, Parr R.G, Development of the Colle-Salvetti correlation-energy formula into a functional of the electron density, *Phys Rev B.*, 37 (1988) 785-789.
26. SPARTAN 06, Wavefunction Inc., Irvine CA, USA, 2006.
27. Harway B.G, Introduction to Nuclear Physics and Chemistry. Englewood Cliffs, New Jersey, Prentice-Hall, 1969.

## FIGURE CAPTIONS

**Figure 1.** Optimized structure and bond lengths for EDNA+p system.

**Figure 2.** The ESP charges (esu) on atoms of EDNA+p system.

**Figure 3.** IR spectrum of EDNA and EDNA+p system.

**Figure 4.** Some of the molecular orbital energy level of of EDNA and EDNA+p system.

**Figure 5.** The HOMO and LUMO patterns for the systems considered (B3LYP/6-31++G(d,p)).

**Figure 6.** UV-VIS spectrum of systems presently considered.

**Figure 7.** Optimized structures for the species considered (UB3LYP/6-31++G(d,p)).

**Figure 8.** Bond lengths in the species considered (UB3LYP/6-31++G(d,p) level, hydrogens are omitted).

**Figure 9.** IR spectra of the species considered (UB3LYP/6-31++G(d,p)).

**Figure 10.** UV-VIS spectra of the species considered (UB3LYP/6-31++G(d,p)).

**Figure 11.** Some of the molecular orbital energy spectra of the species considered (UB3LYP/6-31++G(d,p)).